

# A novel route to perovskite lead zirconate titanate from glycolate precursors via the sol–gel process

N. Tangboriboon<sup>a</sup>, A. Jamieson<sup>b</sup>, A. Sirivat<sup>a</sup> and S. Wongkasemjit<sup>a\*</sup>

A perovskite lead zirconate titanate was synthesized by the sol-gel process, using lead glycolate, sodium tris(glycozirconate) and titanium glycolate as the starting precursors. For the mole ratio Pb : Zr : Ti of 1 : 0.5 : 0.5 [Pb(Zr<sub>0.5</sub>Ti<sub>0.5</sub>)O<sub>3</sub>], TGA-DSC thermal analysis indicated that the percentage of ceramic yield was 55.8, close to the calculated chemical composition value of 49.5. The exothermic peak occurred at 268 °C below the theoretical Curie temperature of 400 °C. The pyrolysis of Pb(Zr<sub>0.5</sub>Ti<sub>0.5</sub>)O<sub>3</sub> of the perovskite phase was investigated in terms of calcination temperature and time. The structure obtained was of the tetragonal form when calcined at temperatures below 400 °C; it transformed to the tetragonal and the cubic forms of the perovskite phase on calcination above the Curie temperature, as verified by X-ray data. The lead zirconate titanate synthesized and calcined at 400 °C for 1 h had the highest dielectric constant, the highest electrical conductivity and the dielectric loss tangent of 10 190,  $0.803 \times 10^{-3} (\Omega \cdot \text{m})^{-1}$  and 1.513 at 1000 Hz, respectively. The lead zirconate titanate powder synthesized has potential applications as an electronic material. Copyright © 2008 John Wiley & Sons, Ltd.

**Keywords:** lead zirconate titanate (PZT); lead glycolate precursor; sodium tris (glycozirconate) precursor; titanium glycolate precursor; piezoelectric materials

## Introduction

Lead zirconate titanate, Pb(Zr<sub>x</sub>Ti<sub>1-x</sub>)O<sub>3</sub> (PZT) of the ABO<sub>3</sub> perovskite structure, was discovered as a piezoelectric material in the 1950s. Since then, it has been identified as an important ferroelectric material suitable for a variety of applications: high energy capacitors, nonvolatile memories, ultrasonic sensors, infrared detectors and electrooptic devices.<sup>[1–3]</sup> It may exist as the single-phase mixed compound of ferroelectric PbTiO<sub>3</sub> (Curie temperature  $T_C = 490^\circ\text{C}$ ) or the antiferroelectric PbZrO<sub>3</sub> ( $T_C = 230^\circ\text{C}$ ) in the isomorphous Pb(Zr<sub>x</sub>Ti<sub>1-x</sub>)O<sub>3</sub>, where  $x < 1$ . The phase diagram, as proposed by Jaffe *et al.*<sup>[4]</sup> and still well recognized, reveals the existence of the nearly temperature-independent morphotropic phase boundary MPB at  $x \approx 0.5$ . The MPB separates the rhombohedral Zr-enriched phase from the tetragonal Ti-enriched phase. The dielectric constant, piezoelectric constant and electromechanical coupling coefficient all show pronounced maximum values for the composition corresponding to the MPB.<sup>[5,6]</sup>

Several conventional PZT synthesis methods usually high calcination temperatures to produce the perovskite phase. The calcination inevitably leads to PZT particle coarsening and aggregation, and consequently nonuniform microstructure and poor electrical properties of PZT. To alleviate this problem, wet-chemistry-based processes were chosen to prepare PZT powders at a lower temperature than the solid-state reaction process. These chemical processes include the co-precipitation, the sol–gel process and the hydrothermal process. Among these methods, the sol–gel process has been widely viewed as a promising one because of the product uniformity at the molecular level and its low operating temperature. However, the sol–gel process has several disadvantages when employed to prepare PZT ceramics in large quantities: it requires a large quantity of solvent and it is very

time-consuming.<sup>[7]</sup> Mandal and Ram synthesized PbZr<sub>0.7</sub>Ti<sub>0.3</sub>O<sub>3</sub> nanoparticles possessing a new tetragonal crystal structure with a polymeric precursor and polyvinyl alcohol.<sup>[1]</sup> Zhang *et al.*<sup>[7]</sup> prepared PZT ceramics derived from a hybrid method between the sol–gel process and the solid-state reaction. Reaction of the oxides to PZT occurred at temperatures as low as 500 °C, and is believed to be induced by the PZT crystallized from the sol–gel portion in the system. Junmin *et al.*<sup>[3]</sup> synthesized lead zirconate titanate from an amorphous precursor by mechanical activation. The resulting PZT powder was well dispersed and the particle size was in the range of 30–50 nm, as observed by SEM and TEM. The dielectric constant measured at 1 kHz was as high as 9100 along with the Curie temperature of 380 °C for PZT sintered at 1150 °C for 1 h and mechanically activated for 20 h.

From these previous studies, the sol–gel process appears to be an alternative method to produce lead zirconate titanate Pb(Zr<sub>x</sub>Ti<sub>1-x</sub>)O<sub>3</sub> (PZT) of ABO<sub>3</sub> perovskite structure from lead, titanium and zirconium (IV) alkoxide precursors, although these precursors are moisture sensitive. Wongkasemjit and co-workers<sup>[8–10]</sup> have demonstrated that, using the oxide one pot synthesis (OOPS) process, moisture-stable metal alkoxides can be successfully synthesized. Therefore, the objective of our study was to synthesize high-purity lead zirconate titanate Pb(Zr<sub>x</sub>Ti<sub>1-x</sub>)O<sub>3</sub> via the sol–gel

\* Correspondence to: S. Wongkasemjit, The Petroleum and Petrochemical College, Chulalongkorn University, Bangkok 10330, Thailand.  
E-mail: dsujitra@chula.ac.th

a The Petroleum and Petrochemical College, Chulalongkorn University, Bangkok 10330, Thailand

b The Macromolecular Science Department, Case Western Reserve University, Cleveland, Ohio, USA

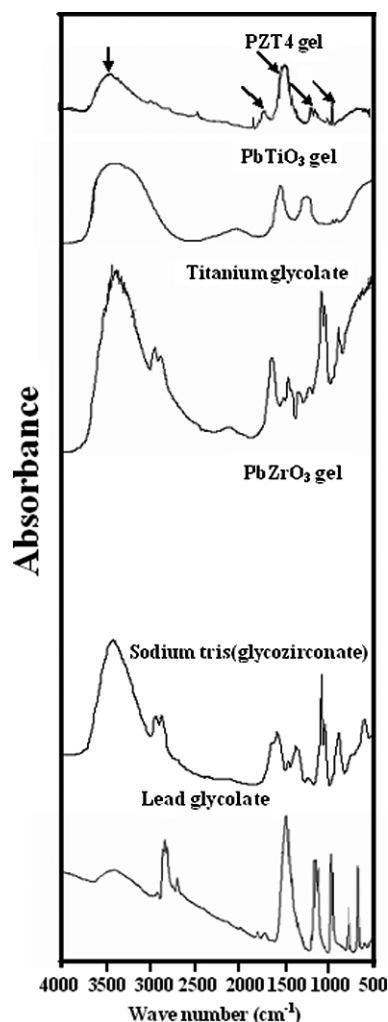


**Figure 1.** FTIR spectra: lead glycolate precursor; titanium glycolate precursor; sodium tris (glycozirconate) precursor,  $\text{PbTiO}_3$  dried gel,  $\text{PbZrO}_3$  dried gel and lead zirconate titanate PZT4 dried gel.

process using lead glycolate,<sup>[10]</sup> titanium glycolate<sup>[9]</sup> and sodium tris(glycozirconate)<sup>[8]</sup> as the moisture-stable precursors. In our work, PZT sols were prepared by mixing lead glycolate, titanium glycolate and sodium tris(glycozirconate) at Pb : Zr : Ti mole ratios of 1 : 0.2 : 0.8, 1 : 0.3 : 0.7, 1 : 0.4 : 0, 1 : 0.5 : 0.5, 1 : 0.6 : 0.4, 1 : 0.7 : 0.3 and 1 : 0.8 : 0.2. The mixtures were then dried and calcined to form PZT powders. We investigated the influences of calcination temperature and time on morphology, electrical properties and the phase transformation.

## Experimental

### Materials

The starting raw materials were lead glycolate, titanium glycolate and sodium tris (glycozirconate) as required OOPS process,<sup>[8–10]</sup> which yields less moisture-sensitive products.

UHP-grade nitrogen, 99.99% purity, was obtained from Thai Industrial Gases Public Company Limited (TIG). Lead acetate trihydrate  $\text{Pb}(\text{CH}_3\text{COO})_2 \cdot 3\text{H}_2\text{O}$ , 99.5% purity, was purchased from Asia Pacific Specialty Chemical Limited (Australia). Titanium dioxide was purchased from Sigma-Aldrich Chemical Co. Ltd

(USA). Zirconium (IV) hydroxide  $\text{Zr}(\text{OH})_4$  containing 88.8%  $\text{ZrO}_2$  purity was purchased from Sigma-Aldrich Chemical Co. Ltd (USA). Sodium hydroxide NaOH of 98% purity was obtained from Asia Pacific Specialty Chemicals Inc. Ltd, and used as received. Ethylene glycol (EG) was purchased from Farmitalia Carlo Erba (Barcelona) or Malinkrodt Baker Inc. (USA), and purified by a fractional distillation under nitrogen at atmosphere pressure and 200 °C before use. Triethylenetetramine (TETA) was purchased from Facai Polytech. Co. Ltd (Thailand) and distilled under vacuum (0.1 mmHg) at 130 °C prior to use. Acetonitrile, HPLC-grade, was purchased from Lab-Scan Co. Ltd.

### Instrumental

The positive fast atom bombardment mass spectra (Maldi-tof-MS) were recorded with a Bruker Instrument (Bruker, Polymer TOF) using sinapinic acid as a matrix, a cesium gun as indicator and cesium iodide (CsI) as a standard for peak calibration. An elemental analyzer was used to determine CHNS/O compositions (Perkin Elmer, PE 2400 Series II) through pyrolysis. Fourier transform infrared spectra (FTIR) were obtained from a spectrometer (Bruker, Vector 3.0) with a spectral resolution of 4  $\text{cm}^{-1}$ . Thermal

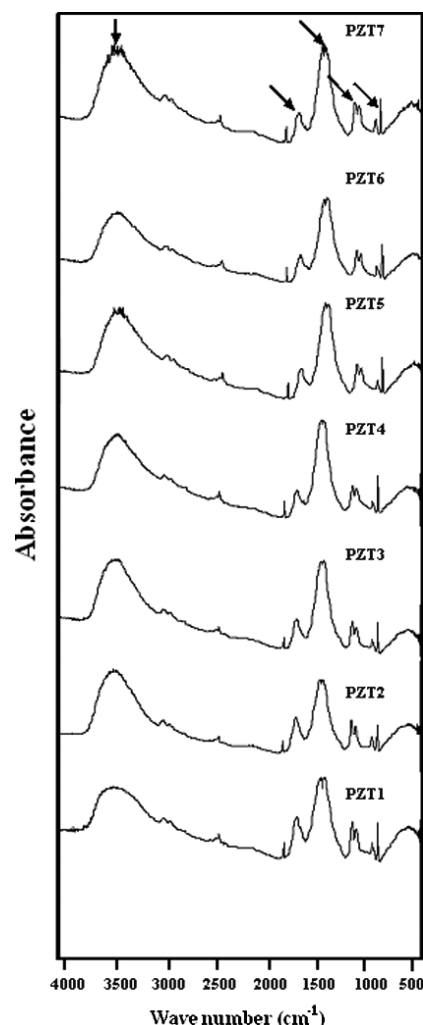


**Figure 2.** FTIR spectra of the lead zirconate titanate dried gels at various mole ratios Pb : Zr : Ti, PZT1 (1 : 0.2 : 0.8), PZT2 (1 : 0.3 : 0.7), PZT3 (1 : 0.4 : 0.6), PZT4 (1 : 0.5 : 0.5), PZT5 (1 : 0.6 : 0.4), PZT6 (1 : 0.7 : 0.3), PZT7 (1 : 0.8 : 0.2).

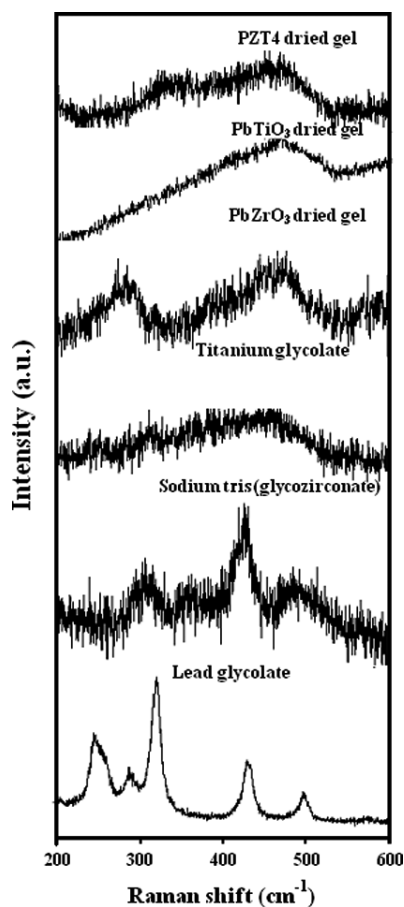


**Figure 3.** Raman spectra of lead glycolate precursor; sodium tris (glyco zirconate) precursor; titanium glycolate precursor; PbZrO<sub>3</sub> dried gel; PbTiO<sub>3</sub> dried gel; and PZT4 dried gel.

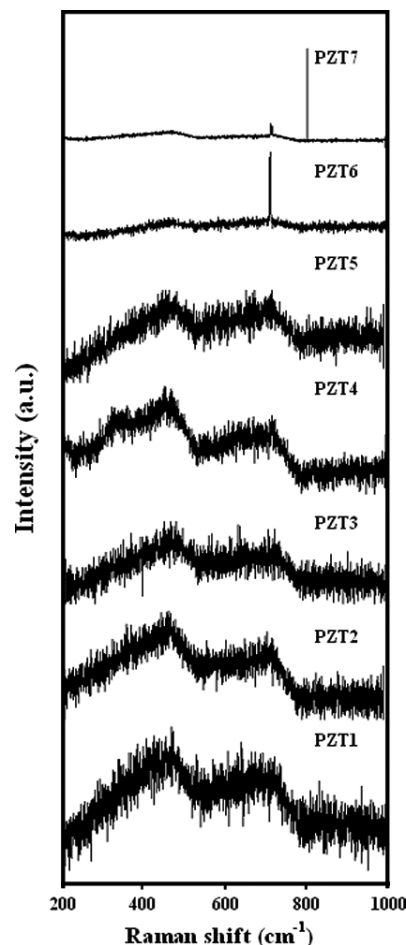


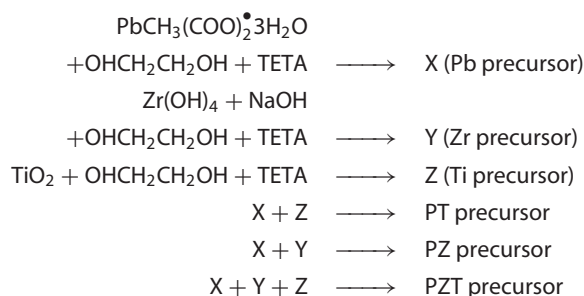
**Figure 4.** Raman spectra of PZT1, PZT2, PZT3, PZT4, PZT5, PZT6 and PZT7.

gravimetric analysis (TGA) and a differential thermal analysis (DTA) were carried out using a thermal analyzer (Perkin Elmer, TG 7) with a heating rate of 10 °C/min over a 25–1200 °C temperature range. The Raman spectra of powder samples were obtained using a spectrometer (Labram HR 800, DU-420-OE-322). X-ray diffraction patterns (XRD) were taken and analyzed using an X-ray analyzer (Philips, N.V.) consisting of CuK $\alpha$  radiation ( $\lambda = 0.154$  nm). Micrographs were obtained using a scanning electron microscope (Jeol, 5200) equipped with EDS for X-ray microanalysis. The percentages of chemical compositions of calcined samples were obtained by an X-ray analytical microscope (Horiba, XGT 2000w). Electrical properties were measured using an impedance analyzer (HP, 4284A).

### Sol–gel process of lead zirconate titanate

Sodium tris (glycozirconate), titanium glycolate, and lead glycolate were synthesized via the OOPS processes which have been previously reported.<sup>[8–10]</sup> The sol–complex alkoxide mixture was prepared by mixing lead glycolate in a 0.1 M nitric solution (HNO<sub>3</sub>) with titanium glycolate and sodium tris (glycozirconate) with Pb:Zr:Ti mole ratios of PZT 1 (1:0.2:0.8), PZT 2 (1:0.3:0.7), PZT 3 (1:0.4:0.6), PZT 4 (1:0.5:0.5), PZT 5 (1:0.6:0.4), PZT 6 (1:0.7:0.3) and PZT 7 (1:0.8:0.2). White turbid solutions were obtained. The sol to gel transition occurred within a few seconds when a small amount of water was added to adjust pH to 9–10 at room

temperature. The gels were allowed to settle at room temperature and kept at 50 °C for 2 days to finally obtain a light yellow gel. The gels were then calcined at 200, 300, 400, 500, 600, 700 and 800 °C for durations of 1, 2 and 3 h. The following six equations summarize our work on the synthesis and the preparations of PT, PZ, and PZT ceramics:



### Electrical properties characterization

The samples were prepared according to the ASTM B263-94 standard for electrical property measurements. Pellet samples were prepared as thin disks 12 mm in diameter and 0.50 mm in thickness. In our experiment, the electrical properties, the dielectric constant, tan delta and electrical conductivity were measured in the frequency range between 10<sup>3</sup> and 10<sup>6</sup> Hz and at room temperature.<sup>[6,11,12]</sup>

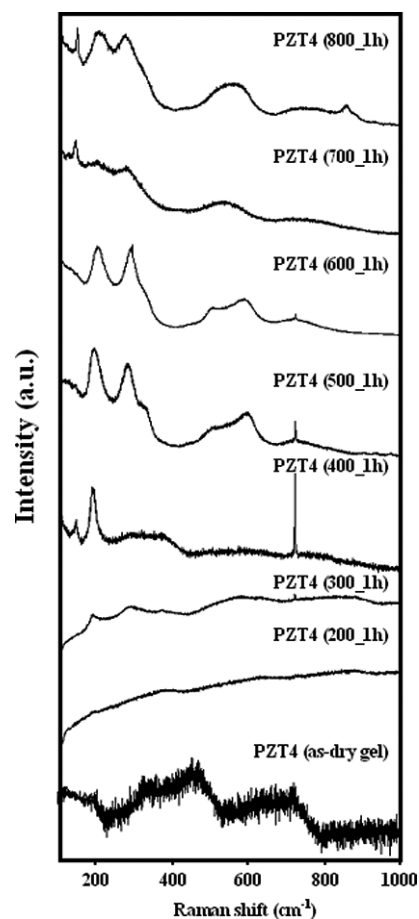


**Figure 5.** Raman spectra of lead zirconate titanate PZT4 dried gel, and calcined lead zirconate titanates at 200, 300, 400, 500, 600, 700 and 800 °C for 1 h.

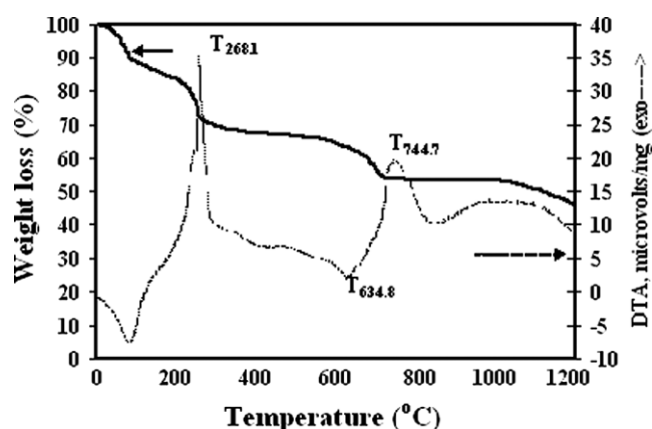


**Figure 6.** TGA-DSC thermograms of lead zirconate titanate PZT4 dried gel from 25 to 1200 °C.

## Results and Discussion

### Characterization of lead zirconate titanate gel and calcined lead zirconate titanate

Figure 1 shows FTIR spectra of lead glycolate, sodium tris(glycozirconate) and titanium glycolate precursors  $\text{PbZrO}_3$ ,  $\text{PbTiO}_3$  and PZT4 dried gels. FTIR spectrum peaks of lead glycolate, sodium tris(glycozirconate) and titanium glycolate precursors have

been identified previously.<sup>[8–10]</sup> The FTIR spectrum of PZT4 dried gel shows a visible broad peak at  $3500\text{ cm}^{-1}$  ( $\nu\text{ O-H}$ ),<sup>[2]</sup> smaller peaks at  $1725$  and  $1630\text{ cm}^{-1}$  ( $\nu\text{ C-O}$ ) and a peak at  $1085\text{ cm}^{-1}$  ( $\nu\text{ C-O-Pb}$ ).<sup>[13,14]</sup> The broad peak at  $783\text{ cm}^{-1}$  can be identified as the  $\text{Pb-O-Zr}$  stretching.<sup>[2,13,14]</sup> These peaks are identical to those of  $\text{PbZrO}_3$  and  $\text{PbTiO}_3$  dried gels, indicating the  $\text{Pb-O-Ti}$  and  $\text{Pb-O-Zr}$  stretchings. The proposed PZT structure in Table 2 suggests that the peaks and the stretchings must be present. Figure 2 shows FTIR spectra of lead zirconate titanate dried gels of various mole ratios between lead glycolate, sodium tris (glycozirconate) and titanium glycolate precursors (PZT1, 1 : 0.2 : 0.8; PZT2, 1 : 0.3 : 0.7; PZT3, 1 : 0.4 : 0.6; PZT4, 1 : 0.5 : 0.5; PZT5, 1 : 0.6 : 0.4; PZT6, 1 : 0.7 : 0.3; and PZT7, 1 : 0.8 : 0.2). The absorbance peaks of various PZTs are similar to each other. A visible broad peak appears at  $3500\text{ cm}^{-1}$  ( $\nu\text{ O-H}$ ),<sup>[2]</sup> smaller peaks at  $1725$  and  $1630\text{ cm}^{-1}$  ( $\nu\text{ C-O}$ ), and a peak at  $1085\text{ cm}^{-1}$  ( $\nu\text{ C-O-Pb}$ ).<sup>[13,14]</sup> The broad peak at  $783\text{ cm}^{-1}$  can be identified as the  $\text{Pb-O-Zr}$  stretching.<sup>[2,13,14]</sup> The peaks at  $3500\text{ cm}^{-1}$  ( $\nu\text{ O-H}$ )<sup>[2]</sup> and  $1630\text{ cm}^{-1}$  ( $\nu\text{ C-O}$ )<sup>[13,14]</sup> increase in intensity with increasing mole ratio between titanium glycolate and sodium tris (glycozirconate).

Raman spectra of lead glycolate precursor, sodium tris(glycozirconate) precursor and titanium glycolate precursor have been previously reported.<sup>[8–10]</sup> In Fig. 3, the Raman spectra of lead titanate, lead zirconate and lead zirconate titanate dried gel show broad bands indicating amorphous structures,  $\text{Pb-O-Ti}$  and  $\text{Pb-O-Zr}$  bondings, consistent with those gels observed previously.<sup>[18,19]</sup> In contrast, the Raman spectra of the precursors show relatively distinct peaks. Figure 4 shows Raman spectra of calcined lead zirconate titanate  $\text{Pb}(\text{Zr}_x\text{Ti}_{1-x})\text{O}_3$  of various mole ratios at room temperature. Raman spectra of PZT1–PZT5 show broad bands indicating their amorphous structures. Raman spectra of PZT6 and PZT7, with the highest mole ratios between titanium glycolate and sodium tris (glycozirconate), show two distinct peaks at  $680$  and  $770\text{ cm}^{-1}$ ; they are identified as the tetragonal structure of lead titanate.<sup>[20,21]</sup> Figure 5 shows the Raman spectra of lead zirconate titanate dried gel (PZT4) of mole ratio 1 : 0.5 : 0.5 at room temperature, and PZT4 at calcination temperatures of 200, 300, 400, 500, 600, 700 and 800 °C, and at 1 h. For calcination temperatures between 400 and 600 °C, distinct peaks appear at 200, 300, 600 and 700  $\text{cm}^{-1}$ , indicating that the PZT perovskite phase developed with the tetragonal structure.<sup>[20]</sup> For higher calcination temperatures between 700 and 800 °C, two peaks appear at 550 and 870  $\text{cm}^{-1}$ , indicating crystalline structures which are to be identified by XRD data as the massicot formations of  $\text{PbO}$  and  $\text{PbO}_2$ .

A thermogram of lead zirconate titanate dried gel PZT4, obtained using the TG-DTA technique, at temperatures between 25 and 1200 °C, is shown in Fig. 6. The weight loss of lead zirconate titanate PZT4 dried gel is 44.2%; the percentage ceramic yield obtained is 55.8%, close to the calculated value of 49.5%. The main weight losses occur at 268 and 744 °C by exothermic reactions. The sharp exothermic peak at 268 °C results from the heat of vaporization of EG generated from the hydrolysis. The weight loss at 744 °C occurs through the  $\text{PbO}$  massicot formation. The temperature of 634.8 °C identifies the endothermic reaction of the phase transformation from PZT to lead oxide.

XRD patterns of lead zirconate titanate dried gels  $\text{Pb}(\text{Zr}_x\text{Ti}_{1-x})\text{O}_3$  (PZT1, PZT2, PZT3, PZT4, PZT5, PZT6 and PZT7) at various mole ratios are shown in Fig. 7. The dominant peaks at  $2\theta = 19, 38$  and  $39^\circ$  belong to lead nitrate [ $\text{Pb}(\text{NO}_3)_2$ ] and the peaks at  $2\theta = 29, 39$  and  $42^\circ$  belong to sodium nitrate (nitratine,  $\text{NaNO}_3$ ), in agreement with JCPDS patterns of 36-1462 and 36-1474, respectively. These



were products of the sol–gel process from the additions of nitric acid and sodium hydroxide. The different levels of XRD intensity amongst PZT dried gels reflect the differences in the mole ratio according to Table 1.

XRD patterns of lead zirconate titanate samples calcined at 200, 300, 400, 500, 600, 700 and 800 °C and at calcination

times of 1, 2 and 3 h are shown in Fig. 8. For PZT at calcination temperature of 200 °C, we obtain a small amount of the tetragonal structure  $\text{Pb}(\text{Zr}_{0.5}\text{Ti}_{0.5})\text{O}_3$ . For PZT at a calcination temperature of 300 °C at 1, 2 or 3 h, we obtained a mixture of the tetragonal structure and the lead oxide  $\{\text{Pb}(\text{Zr}_{0.5}\text{Ti}_{0.5})\text{O}_3[\text{tetragonal}] + \text{PbO}[\text{orthorhombic}]\}$ . For PZT at

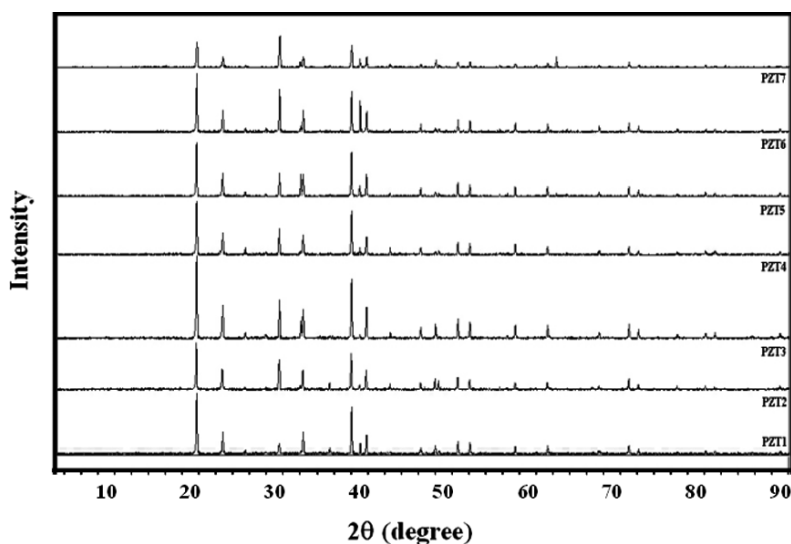


**Figure 7.** XRD diffraction patterns of lead zirconate titanate  $\text{Pb}(\text{Zr}_x\text{Ti}_{1-x})\text{O}_3$  dried gels: PZT1, PZT2, PZT3, PZT4, PZT5, PZT6 and PZT7.

**Table 1.** Lead zirconate titanate dried gels, PZT and calcined lead zirconate titanates PZT4  $\text{Pb}(\text{Zr}_x\text{Ti}_{1-x})\text{O}_3$  of various calcination temperatures and times with corresponding %PbO, %ZrO<sub>2</sub>, %TiO<sub>2</sub> and Pb : Zr : Ti mole ratios

Sample: Pb : Zr : Ti	Color	%PbO	%ZrO <sub>2</sub>	%TiO <sub>2</sub>	Mole ratio Pb : Zr : Ti
PZT1 (1 : 0.8 : 0.2)	Light yellow	74.54	22.31	3.15	1 : 0.822 : 0.178
PZT2 (1 : 0.7 : 0.3)	Light yellow	78.42	17.02	4.56	1 : 0.708 : 0.292
PZT3 (1 : 0.6 : 0.4)	Light yellow	77.37	15.58	7.05	1 : 0.587 : 0.413
PZT4 (1 : 0.5 : 0.5)	Light yellow	76.12	13.98	9.90	1 : 0.479 : 0.521
PZT5 (1 : 0.4 : 0.6)	Light yellow	74.34	13.51	12.15	1 : 0.420 : 0.580
PZT6 (1 : 0.3 : 0.7)	Light yellow	63.51	16.22	20.27	1 : 0.342 : 0.658
PZT7 (1 : 0.2 : 0.8)	Light yellow	77.18	7.74	15.07	1 : 0.250 : 0.750
PZT4 (200_1h)	Dark brown	71.35	13.76	14.89	1 : 0.376 : 0.624
PZT4 (200_2h)	Dark brown	74.57	13.50	11.92	1 : 0.433 : 0.576
PZT4 (200_3h)	Dark brown	65.26	22.65	12.09	1 : 0.549 : 0.451
PZT4 (300_1h)	Brown yellow	72.86	14.49	12.65	1 : 0.427 : 0.573
PZT4 (300_2h)	Brown yellow	68.46	17.39	14.16	1 : 0.444 : 0.556
PZT4 (300_3h)	Brown yellow	72.47	17.49	10.04	1 : 0.531 : 0.469
PZT4 (400_1h)	Dark yellow	67.83	18.55	13.62	1 : 0.531 : 0.469
PZT4 (400_2h)	Dark yellow	70.83	16.78	12.39	1 : 0.468 : 0.532
PZT4 (400_3h)	Dark yellow	73.68	15.62	10.70	1 : 0.487 : 0.513
PZT4 (500_1h)	Dark yellow	70.14	18.69	11.17	1 : 0.521 : 0.479
PZT4 (500_2h)	Dark yellow	73.90	15.67	10.43	1 : 0.493 : 0.507
PZT4 (500_3h)	Dark yellow	71.43	16.82	11.74	1 : 0.482 : 0.518
PZT4 (600_1h)	Orange yellow	74.89	12.00	13.10	1 : 0.373 : 0.627
PZT4 (600_2h)	Orange yellow	73.44	14.01	12.56	1 : 0.420 : 0.580
PZT4 (600_3h)	Orange yellow	69.91	15.73	14.36	1 : 0.416 : 0.584
PZT4 (700_1h)	Yellow	69.12	19.84	11.05	1 : 0.539 : 0.461
PZT4 (700_2h)	Yellow	70.57	11.76	17.67	1 : 0.302 : 0.698
PZT4 (700_3h)	Yellow	62.59	19.76	17.66	1 : 0.421 : 0.579
PZT4 (800_1h)	Light yellow	55.36	18.14	26.50	1 : 0.308 : 0.692
PZT4 (800_2h)	Light yellow	77.06	9.59	13.35	1 : 0.318 : 0.682
PZT4 (800_3h)	Light yellow	55.56	14.31	30.13	1 : 0.236 : 0.764

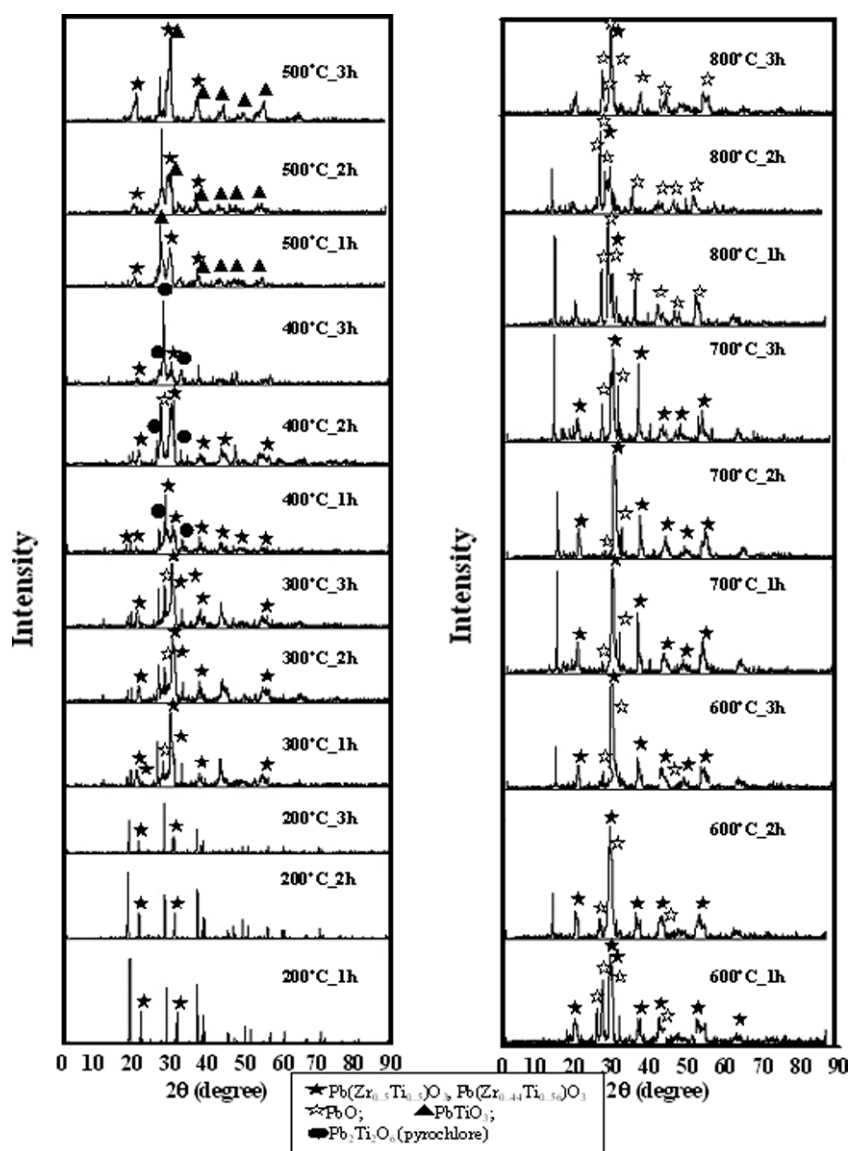


**Figure 8.** XRD diffraction patterns of calcined lead zirconate titanate powders (PZT4) at 200, 300, 400, 500, 600, 700 and 800 °C for durations of 1, 2 and 3 h.

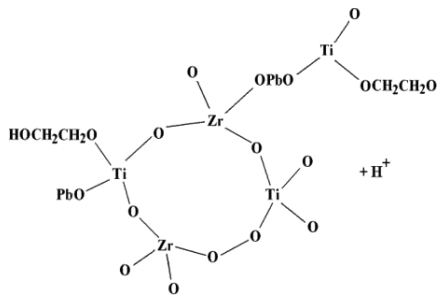
a calcination temperature of 400 °C at 1, 2 or 3 h, we obtained in addition the pyrochlore phase  $\{Pb(Zr_{0.5}, Ti_{0.5})O_3[\text{tetragonal}] + PbO[\text{orthorhombic}] + Pb_2Ti_2O_6\}$ . For PZT at a calcination temperature of 500 °C at 1, 2 and 3 h, we obtained a mixture of the tetragonal structure and the cubic lead titanate structure  $\{Pb(Zr_{0.5}, Ti_{0.5})O_3[\text{tetragonal}] + PbTiO_3[\text{cubic}]\}$ .<sup>[6]</sup> For PZT at calcination temperatures of 600 and 700 °C at 1, 2 or 3 h, we obtained the cubic structure and lead oxide  $\{Pb(Zr_{0.5}, Ti_{0.5})O_3[\text{cubic}] + PbO[\text{cubic and orthorhombic}] + PbO_2[\text{cubic}]\}$ . Finally, for PZT at calcination temperature of 800 °C at 1, 2 or 3 h, we obtained the cubic structures  $\{Pb(Zr_{0.5}, Ti_{0.5})O_3[\text{cubic}] + PbO_2[\text{cubic}]\}$ . At the calcination temperatures of 700 and 800 °C, the massicot formations of PbO and PbO<sub>2</sub> correspond to the Raman peaks of 550 and 870  $\text{cm}^{-1}$ , as shown in Fig. 3. In summary, the peaks in Fig. 8 are consistent with those of the International Center for Diffraction Data Standard (JCPDS) patterns of lead titanium zirconium oxide, tetragonal form (14-0031), lead oxide, massicot phase, orthorhombic form (38-1477), lead titanate, cubic form (40-0099),

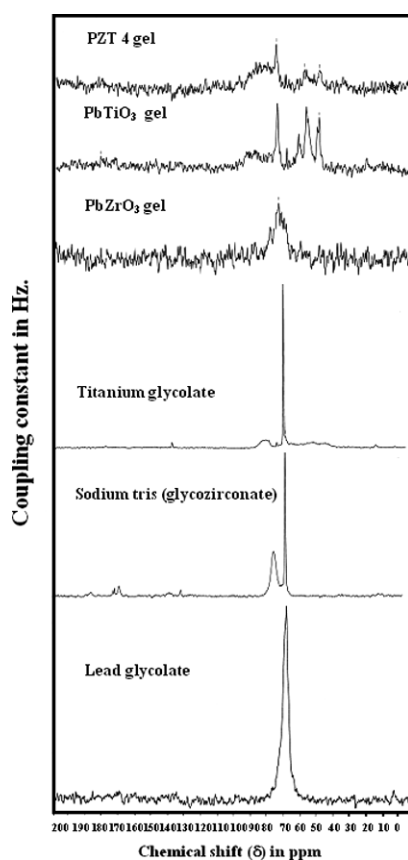
lead titanate zirconate, tetragonal form (50-0346) and lead titanium oxide, metastable (26-0142).<sup>[2,6,7]</sup>

<sup>13</sup>C-NMR spectra of lead glycolate, sodium tris (glycozirconate), titanium glycolate, lead zirconate dried gel, lead titanate dried gel and lead zirconate titanate dried gel are shown in Fig. 9. All of spectra commonly show the peak of ethylene glycol ligand at 69 ppm, consistent with previously reported data<sup>[8–10,14]</sup> and the proposed structure in Table 2.

SEM micrographs at the magnification of 350 show microstructures of PZT4 dried gel [Fig. 10(a)] and calcined PZT4 [Fig. 10(b)–(h)]. Lead zirconate titanate particles become agglomerated starting at 200 °C, as shown in Fig. 10(b). The PZT4 particles [Fig. 10(b)–(e)] appear to be soft when the calcinations temperature is below the Curie temperature of 490 °C; they are more brittle at higher temperatures [Fig. 10(f)–(h)]. In general, particle shapes are quite irregular and sizes are nonuniform. These results may reflect the fact that we obtain different structures depending on the calcinations temperature, consistent with the XRD data.

**Table 2.** The proposed structure and the percentage of carbon content of the lead zirconate titanate PZT4 dried gel

m/e	Proposed structure	% carbon content (experimental)	% carbon content (calculated chemical composition)
1085		$4.548 \pm 0.101$	4.421

**Figure 9.**  $^{13}\text{C}$ -Solid state NMR spectra of the synthesized lead glycolate precursor, sodium tris(glycozirconate) precursor, titanium glycolate precursor,  $\text{PbZrO}_3$  dried gel,  $\text{PbTiO}_3$  dried gel and PZT4 dried gel.

The chemical composition percentages of calcined samples were analyzed by an X-ray analytical microscope and the data are given in Table 1. The experimental mole ratio of  $\text{PbO}:\text{ZrO}_2:\text{TiO}_2$  of 1.00:0.521:0.479 is close to the theoretically calculated mole ratio of the lead zirconate titanate  $\text{Pb}(\text{Zr}_{0.5}\text{Ti}_{0.5})\text{O}_3$  or PZT4, which is 1.00:0.500:0.500. From the elemental analysis, data were used to calculate the percentage of carbon, which turns out to be  $4.548 \pm 0.101$ , a value close to theoretically calculated chemical composition of 4.424. From the mass spectroscopy, we obtained

a molecular weight of 1085 g/mol for our calcined samples. Based on these data, we propose a possible structure as shown in Table 2.

### Electrical properties of lead zirconate titanate

Figure 11 shows the dielectric constants and dielectric loss tangents of the starting precursors, lead zirconate dried gel, lead titanate dried gel, and lead zirconate titanate dried gel (PZT4) as functions of frequency at  $27^\circ\text{C}$ . The lead titanate dried gel possesses the highest dielectric constant at  $10^3$  Hz and the highest loss tangent; namely, 1150 and  $4.262.76 \times 10^{-4}$  S/m, respectively. It also has the highest electrical conductivity value of  $2.76 \times 10^{-4}$  at  $10^3$  Hz (Table 3). Corresponding values for other materials are tabulated in Table 3. In Fig. 11, we can observe that the dielectric constants and the dielectric loss tangents of the starting precursors and the dried gels generally decrease with increasing frequency, indicative of the polarization mechanisms involved: the electronic, atomic, the dipole and the interfacial polarizations.<sup>[15]</sup>

Figures 12 shows the dielectric constants and the dielectric loss tangents of lead zirconate titanate dried gels  $\text{Pb}(\text{Zr}_x\text{Ti}_{1-x})\text{O}_3$  (PZT1, PZT2, PZT3, PZT4, PZT5, PZT6 and PZT7) as functions of frequency and at  $27^\circ\text{C}$ . Amongst various mole ratios of  $\text{Pb}:\text{Zr}:\text{Ti}$  of  $\text{Pb}(\text{Zr}_x\text{Ti}_{1-x})\text{O}_3$ ,  $\text{Pb}(\text{Zr}_{0.5}\text{Ti}_{0.5})\text{O}_3$  or PZT4 possesses the highest dielectric constant, nearly the highest loss tangent and the highest electrical conductivity values at frequencies between  $10^3$  and  $10^6$  Hz. In particular at  $10^3$  Hz, PZT4 dried gel possesses the dielectric constant, the dielectric loss tangent and the electrical conductivity values of 9.832 and 0.405, and  $9.98 \times 10^{-8}$  S/cm, respectively. Table 3 lists the dielectric constant, the dielectric loss tangent and the electrical conductivity values at  $10^3$  Hz at  $27^\circ\text{C}$  of all the lead zirconate titanate dried gels investigated

Table 3 also lists the dielectric constant, the dielectric loss tangent and the electrical conductivity values at 1000 Hz and at  $27^\circ\text{C}$  of the calcined lead zirconate titanate samples  $\text{Pb}(\text{Zr}_{0.5}\text{Ti}_{0.5})\text{O}_3$  at various calcination temperatures and times. Among these samples, it can be seen that  $\text{Pb}(\text{Zr}_{0.5}\text{Ti}_{0.5})\text{O}_3$  400-1 h, the lead zirconate titanate calcined at  $400^\circ\text{C}$  for a duration of 1 h, possesses the highest dielectric constant of 10 190, with corresponding dielectric loss tangent of 1.513, and the highest DC electrical conductivity of  $0.803 \times 10^{-3}$  S/m. This calcined sample corresponds to the purest tetragonal structure of the perovskite phase along with a small amount of pyrochlore phase, as shown previously from the X-ray data of Fig. 8. With the tetragonal structure of the perovskite phase, we may expect the ferroelectric and the piezoelectric properties.<sup>[16]</sup> At higher calcination temperatures, above

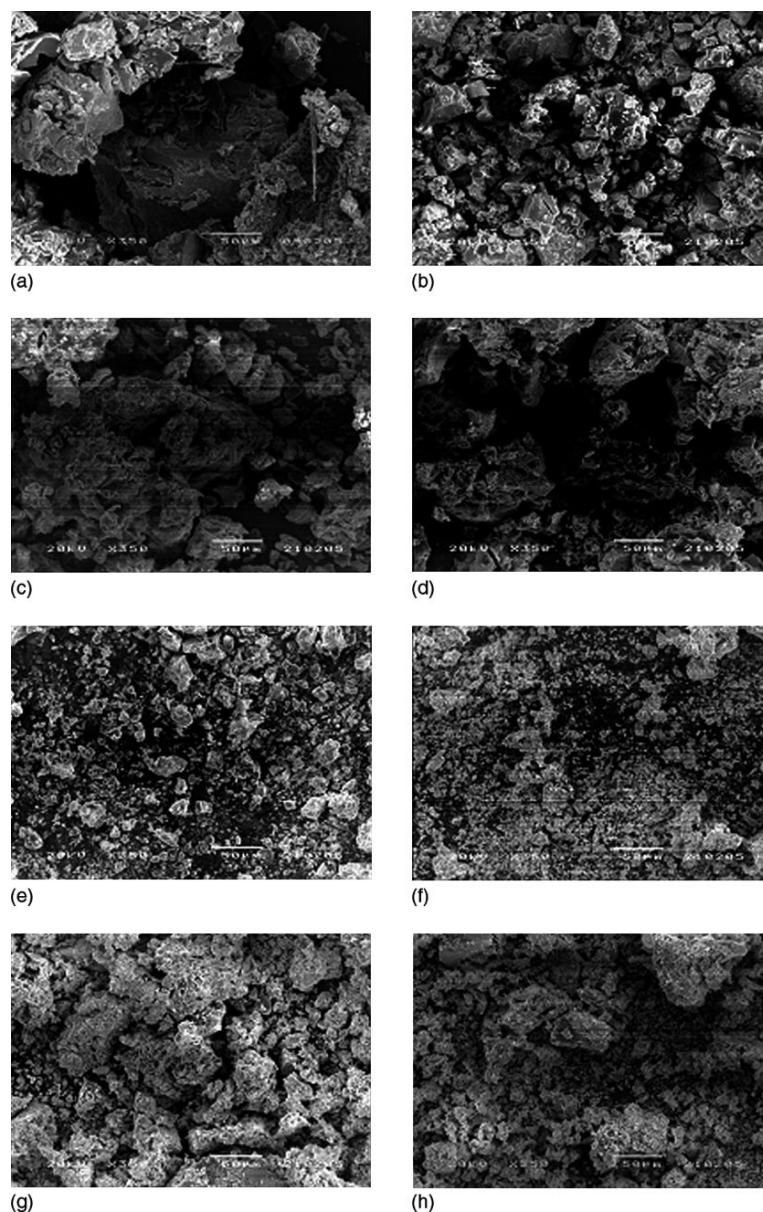


**Figure 10.** SEM micrographs showing microstructure of PZT4 dried gel and calcined PZT4 at: (a) dried gel 25 °C; (b) 200 °C; (c) 300 °C; (d) 400 °C; (e) 500 °C; (f) 600 °C; (g) 700 °C; and (h) 800 °C for 1 h at the magnification of 350.

the Curie temperature of  $\text{Pb}(\text{Zr}_{0.5}\text{Ti}_{0.5})\text{O}_3$  of 400 °C, we may expect both the dielectric constant and the electrical conductivity to decrease with increasing calcination temperature since the structures become more of the cubic form, which is accompanied by paraelectricity.<sup>[16]</sup>

Figure 13 shows the dielectric constants and the dielectric loss tangents of the calcined lead zirconate titanate  $\text{Pb}(\text{Zr}_{0.5}\text{Ti}_{0.5})\text{O}_3$  or PZT4 of various frequencies at functions of calcination temperature. For PZT4, its dielectric constant and dielectric loss tangent increase initially with calcination temperature and reach maximum values at 400 °C and then decrease at higher calcination temperatures. The maximum dielectric constant and dielectric loss values obtained are 10 190 and 1.513, respectively; the maxima are expected to occur close to the Curie temperature of 400 °C. We may compare our data of our synthesized  $\text{Pb}(\text{Zr}_{0.5}\text{Ti}_{0.5})\text{O}_3$  or PZT4 with the data from other

workers, who obtained dielectric constant values of 8600<sup>[17]</sup> and 1050,<sup>[7]</sup> measured at 1000 Hz and at room temperature, respectively.

## Conclusions

Our synthesis of lead zirconate titanate by the sol–gel process using lead glycolate, sodium tris (glycozirconate) and titanium glycolate as starting precursors gave a high-purity and low-moisture-sensitivity light yellow powder. The experimental stoichiometry value between  $\text{PbO}$ ,  $\text{ZrO}_2$  and  $\text{TiO}_2$  was 1.00:0.521:0.479, close to the calculated value of  $\text{PbZrO}_3$ . The lead zirconate titanate gel was dried and calcined below the Curie temperature to prevent structural change from the tetragonal or the orthorhombic forms to the cubic form in the perovskite phase. The highest dielectric constant of 10 190, electrical conductivity of  $0.803 \times 10^{-3} (\Omega \text{ m})^{-1}$



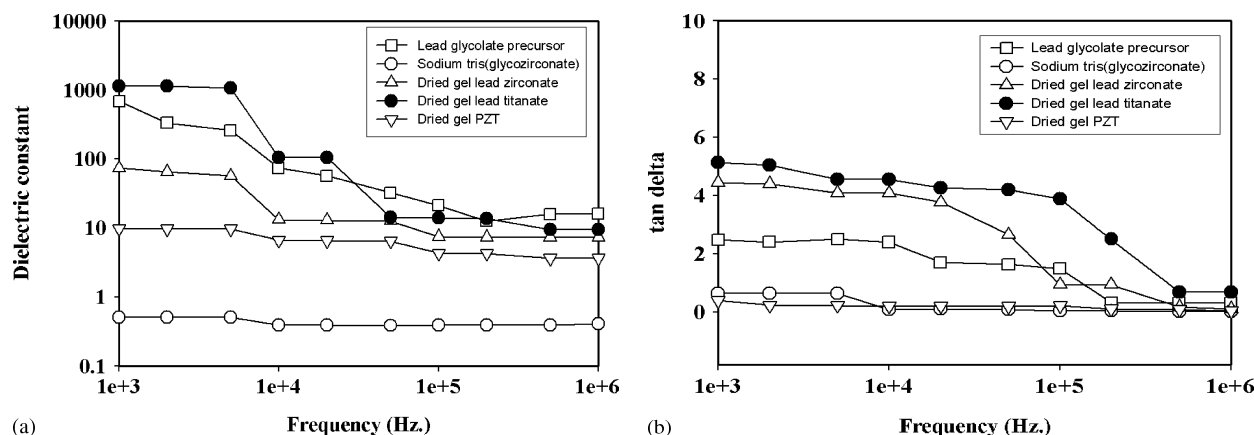


**Figure 11.** Dielectric constant and  $\tan\delta$  of lead glycolate precursor, sodium tris(glycozirconate) precursor, lead zirconate dried gel, lead titanate dried gel and lead zirconate titanate (PZT4) dried gel vs frequency measured at room temperature.

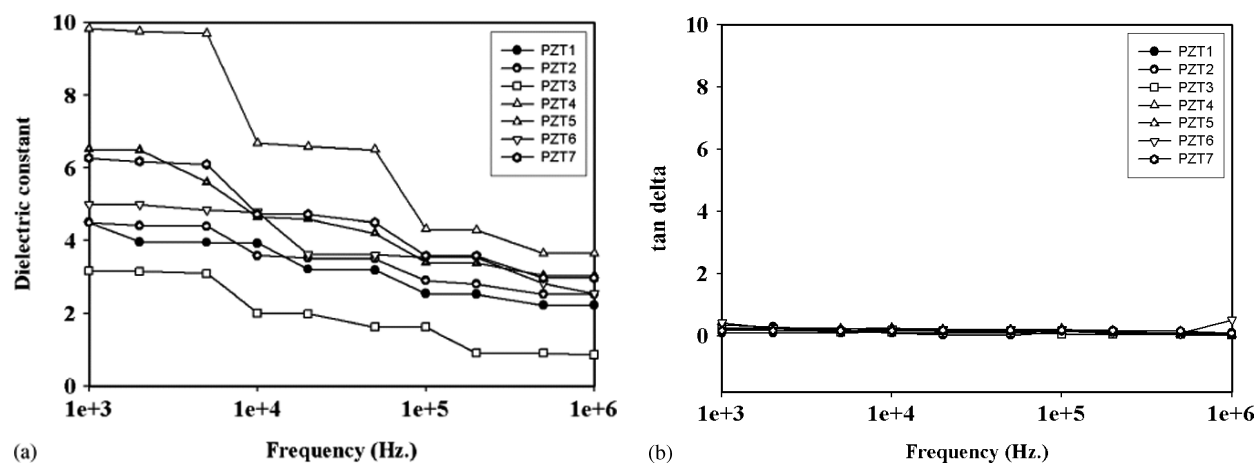


**Figure 12.** Dielectric constant and  $\tan\delta$  of lead zirconate titanate  $\text{Pb}(\text{Zr}_x\text{Ti}_{1-x})\text{O}_3$  dried gels: PZT1, PZT2, PZT3, PZT4, PZT5, PZT6 and PZT7 vs frequency measured at room temperature.

and low dielectric loss tangent of 1.513 measured at 1000 Hz were obtained with  $\text{Pb}(\text{Zr}_{0.5}\text{Ti}_{0.5})\text{O}_3$  calcined at 400 °C for 1 h. Dielectric constant and conductivity decreased with calcination time and temperature when it was above the Curie temperature. Our synthesized materials appear to be suitable candidates for an electronic-grade  $\text{Pb}(\text{Zr}_{0.5}\text{Ti}_{0.5})\text{O}_3$ .

## Acknowledgments

The authors would like to thank the Center of Excellence in Petroleum Petrochemicals and Advanced Materials, the Ratchadapisek Sompoch Fund of Chulalongkorn University and the Faculty of Engineering, Kasetsart University for financial sup-

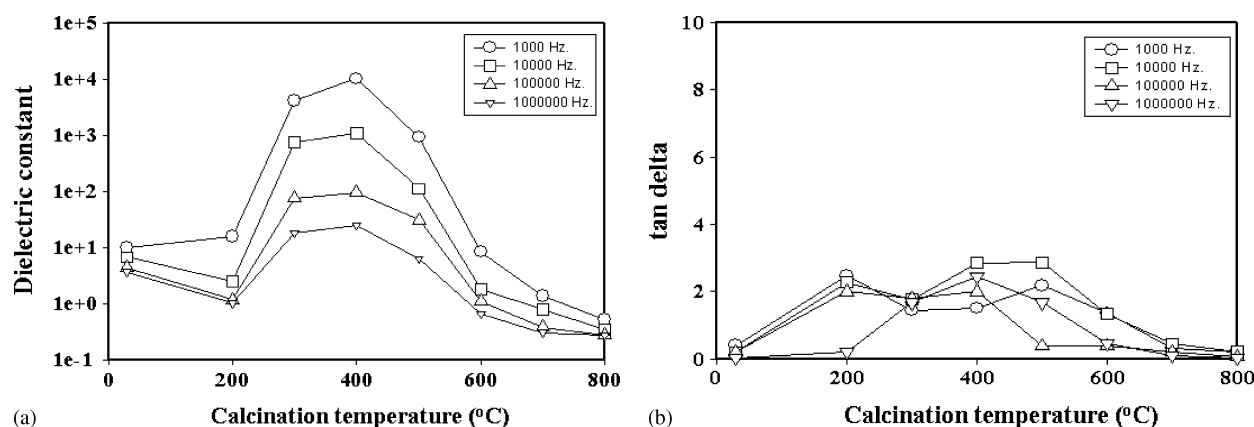


**Figure 13.** Dielectric constant and  $\tan\delta$  of calcined lead zirconate titanate  $\text{Pb}(\text{Zr}_x\text{Ti}_{1-x})\text{O}_3$  (PZT4) vs calcination temperature (200, 300, 400, 500, 600, 700 and 800 °C) for 1 h at various frequencies.

**Table 3.** The dielectric properties (1000 Hz, 27 °C) and DC electrical conductivity of lead glycolate precursor, sodium tris(glycozirconate) precursor, titanium glycolate precursor, lead zirconate titanate of  $\text{Pb}(\text{Zr}_x\text{Ti}_{1-x})\text{O}_3$  dried gels PZT1, PZT2, PZT3, PZT4, PZT5, PZT6 and PZT7 and calcined lead zirconate titanates PZT4 of various calcination temperatures and times

Sample	Dielectric constant	Dielectric loss tangent ( $\tan\delta$ )	Conductivity ( $\Omega\cdot\text{m}$ ) <sup>-1</sup>
Lead glycolate precursor	691.70	2.481	$8.850 \times 10^{-5}$
Sodium tris (glycozirconate) precursor	0.507	0.635	$1.781 \times 10^{-8}$
Titanium glycolate precursor	15.70	1.831	$1.390 \times 10^{-6}$
Lead titanate dried gel	1150	4.261	$2.76 \times 10^{-4}$
Lead zirconate dried gel	73.76	4.448	$1.516 \times 10^{-4}$
Dried gel PZT1	4.496	0.354	$6.450 \times 10^{-8}$
Dried gel PZT2	4.501	0.084	$2.650 \times 10^{-8}$
Dried gel PZT3	3.165	0.236	$1.920 \times 10^{-8}$
Dried gel PZT4	9.832	0.405	$9.980 \times 10^{-8}$
Dried gel PZT5	6.522	0.232	$8.700 \times 10^{-8}$
Dried gel PZT6	4.997	0.419	$6.620 \times 10^{-8}$
Dried gel PZT7	6.273	0.163	$4.690 \times 10^{-8}$
PZT4 (200_1h)	15.49	2.473	$3.055 \times 10^{-5}$
PZT4 (200_2h)	12.43	2.350	$9.210 \times 10^{-5}$
PZT4 (200_3h)	429.9	2.588	$4.430 \times 10^{-5}$
PZT4 (300_1h)	2613	1.437	$3.210 \times 10^{-5}$
PZT4 (300_2h)	2817	1.232	$1.940 \times 10^{-4}$
PZT4 (300_3h)	4088	1.356	$1.840 \times 10^{-4}$
PZT4 (400_1h)	10 190	1.513	$0.803 \times 10^{-3}$
PZT4 (400_2h)	1922.3	1.370	$0.646 \times 10^{-4}$
PZT4 (400_3h)	1936.0	1.866	$1.970 \times 10^{-4}$
PZT4 (500_1h)	907.3	2.182	$1.050 \times 10^{-4}$
PZT4 (500_2h)	602.7	1.507	$2.280 \times 10^{-4}$
PZT4 (500_3h)	602.5	1.834	$0.820 \times 10^{-6}$
PZT4 (600_1h)	8.275	1.376	$7.040 \times 10^{-6}$
PZT4 (600_2h)	0.8987	0.311	$1.540 \times 10^{-7}$
PZT4 (600_3h)	0.2350	0.552	$0.730 \times 10^{-7}$
PZT4 (700_1h)	1.3520	0.320	$2.360 \times 10^{-7}$
PZT4 (700_2h)	1.0820	0.310	$1.850 \times 10^{-7}$
PZT4 (700_3h)	1.2690	0.315	$2.198 \times 10^{-7}$
PZT4 (800_1h)	0.5116	0.227	$6.410 \times 10^{-8}$
PZT4 (800_2h)	0.6769	0.615	$0.227 \times 10^{-8}$
PZT4 (800_3h)	0.6360	0.456	$0.162 \times 10^{-8}$

port, and the Department of Materials Engineering, the Chemistry Department and the Physics Department, Kasetsart University, for the X-ray diffraction and electrical property measurements. A.S. would like to acknowledge the partial financial supports from the Conductive and Electroactive Polymers Research Unit and KFAS, both of Chulalongkorn University, Thailand Research Fund (BRG 5080029), and the Royal Thai Government (Budget of Fiscal Year 2550).

## References

- [1] Mandal T. K, Ram S. *Mater. Lett.* 2003; **57**: 2432.
- [2] Tipakontitkul R, Ananta S. *Mater. Lett.* 2004; **58**: 449.
- [3] Junmin X, Wang J, Weiseng T. *J. All. Com.* 2000; **308**: 139.
- [4] Jaffe B, Roth RS, Marzullo S. *J. Appl. Phys.* 1954; **25**: 809.
- [5] Misra SK, Singh AP, Pandey D, Mag P. *Phil. Mag. B* 1997; **76**: 213.
- [6] Kong LB, Ma J. *Mater. Lett.* 2001; **51**: 95.
- [7] Zhang RF, Ma J, Kong LB, Chen YZ, Zhang TS. *Mater. Lett.* 2002; **55**: 388.
- [8] Ksapabutr B, Gulari E, Wongkasemjit S. *Mater. Chem. Phys.* 2004; **83**(1): 14.
- [9] Phonthammachai N, Chairassameewong T, Gulari E, Jamieson A, Wongkasemjit S. *J. Metals. Min. Mater., Chulalongkorn University* 2002; **12**(1): 23.
- [10] Tangboriboon N, Jamieson A, Sirivat A, Wongkasemjit S. *Mater. Chem. Phys.* 2006; **98**: 138.
- [11] Thomas R, Mochizuki S, Mihara T, Ishida T. *Mater. Lett.* 2003; **57**: 2007.
- [12] Las WC, Spagnol PD, Zaghet MA, Cilense M. *Cer. Int.* 2001; **27**: 367.
- [13] AbreuA Jr, Zanetti SM, Oliveira MAS, Thin GP. *J. Eur. Cer. Soc.* 2005; **25**: 743.
- [14] Kakihana M, Okubu T, Arima M, Uchiyama O, Yashima M, Yuchimura M. *Chem. Mater.* 1997; **9**(2): 451.
- [15] Bharadwaja SSN, Krupanidhi SB. *Thin Solid Films* 2001; **391**: 126.
- [16] Deshpande AS, Kholam YB, Patil AJ, Deshpande SB, Potdar HS, Date SK. *Mater. Lett.* 2001; **51**: 161.
- [17] Xu ZJ, Chu RQ, Li GR, Shao X, Yin QR. *Mater. Sci. Engng* 2004; **B117**: 113.
- [18] Bersani D, Lottici PP, Montenero A, Pigoni S, Gnappi G. *J. Non. Cryst. Solid* 1995; **192–193**: 490.
- [19] Camargo ER, Popa M, Frantti J, Kakihana M. *Chem. Mater.*, 2001; **13**: 13943.
- [20] Pontes FM, Leite ER, Nunes MSJ, Pontes DSL, Longo E, Magnani R, Pizani PS, Varela JA. *J. Eur. Cer. Soc.* 2004; **24**: 2969.
- [21] Burns G, and Scott BA. *Phys. Rev. Lett.* 1970; **25**(17): 1191.